

자유표면 시뮬레이션의 TOUD 연구

곽 승 현
한라대학교 시스템응용공학부

Study on the Third-Order-Upwind-Difference(TOUD) for the Free-Surface Simulation

SEUNG-HYUN KWAG

School of Applied System Engineering, Halla University
66 Heungup, Wonju, Kangwondo 220-712 Korea
Email: shkwag@hit.halla.ac.kr, Fax: 033-760-1361

Key Words: Third Order Upwind Difference, Free Surface, Navier-Stokes, Hydrofoil

Abstract: A new finite difference scheme is studied for the simulation of free surface, where the third derivative term for the wave elevation is artificially added in the free-surface boundary condition. This study presents a comparative analysis with simulations performed by using the classical MAC method. More systematic computations are carried out by changing the submergence depth and angle of attack. Through the numerical simulation, it is found that a new numerical method becomes more efficient for the reason that the free surface elevation is reasonably developed at the rear of trailing edge.

1. Introduction

Field discretization methods are most commonly used to solve the Navier-Stokes equations, e.g., the MAC (Marker and Cell) method of Harlow and Welch(1965) and its various improved versions including Nichols & Hirt (1971) and Miyata (1986). A review of this subject may be found in Floryan(1989).

A new finite difference scheme for the calculation of the wave elevation is studied where the third derivative term of the wave elevation is artificially added in the Eulerian expression of the free surface condition. The additional inclusion is attracted by the fact that the third derivative contributes only to the periodic propagation either in the time domain or in the progressive direction.

In the current paper, the third derivative term

was applied to the 3-D body in order to study the feasibility on a new computational method of the free surface elevation. Further systematic computations and studies on the grid size are carried out with a finite difference scheme for the free surface computations.

2. Numerical Scheme

2.1 Governing Equations

The velocity components u , v and w at the next time step are determined by

$$\begin{aligned} u^{n+1} &= (F^n - \phi_x^n) \Delta t \\ v^{n+1} &= (G^n - \phi_y^n) \Delta t \\ w^{n+1} &= (H^n - \phi_z^n) \Delta t \end{aligned} \quad (1)$$

where

$$F^n = \frac{u^n}{\Delta t} + \left(\frac{1}{Re} + \nu \right) \nabla^2 u$$

$$\begin{aligned}
& - \left(u^n \frac{\partial u}{\partial x} + v^n \frac{\partial u}{\partial y} + w^n \frac{\partial u}{\partial z} \right) \\
& - \frac{\partial}{\partial x} \left\{ v_i \left(2 \frac{\partial u}{\partial x} \right) \right\} - \frac{\partial}{\partial y} \left\{ v_i \left(\frac{\partial u}{\partial y} + \frac{\partial v}{\partial x} \right) \right\} \\
& - \frac{\partial}{\partial z} \left\{ v_i \left(\frac{\partial u}{\partial z} + \frac{\partial w}{\partial x} \right) \right\} \\
G^n = & \frac{v^n}{\Delta t} + \left(\frac{1}{Re} + v_i \right) \nabla^2 v \\
& - \left(u^n \frac{\partial v}{\partial x} + v^n \frac{\partial v}{\partial y} + w^n \frac{\partial v}{\partial z} \right) \\
& - \frac{\partial}{\partial x} \left\{ v_i \left(\frac{\partial u}{\partial y} + \frac{\partial v}{\partial x} \right) \right\} - \frac{\partial}{\partial y} \left\{ v_i \left(2 \frac{\partial v}{\partial y} \right) \right\} \\
& - \frac{\partial}{\partial z} \left\{ v_i \left(\frac{\partial v}{\partial z} + \frac{\partial w}{\partial y} \right) \right\}
\end{aligned} \tag{2}$$

$$\begin{aligned}
H^n = & \frac{w^n}{\Delta t} + \left(\frac{1}{Re} + v_i \right) \nabla^2 w \\
& - \left(u^n \frac{\partial w}{\partial x} + v^n \frac{\partial w}{\partial y} + w^n \frac{\partial w}{\partial z} \right) \\
& - \frac{\partial}{\partial x} \left\{ v_i \left(\frac{\partial u}{\partial z} + \frac{\partial w}{\partial x} \right) \right\} - \frac{\partial}{\partial y} \left\{ v_i \left(\frac{\partial v}{\partial z} + \frac{\partial w}{\partial y} \right) \right\} \\
& - \frac{\partial}{\partial z} \left\{ v_i \left(2 \frac{\partial w}{\partial z} \right) \right\}
\end{aligned}$$

and

$$\Phi^n = p + \frac{z}{Fn^2} \tag{3}$$

Differentiating Eq. (1) with respect to x, y and z,

$$\begin{aligned}
\nabla^2 \Phi = & F_x + G_y + H_z \\
& - (u_x^{n+1} + v_y^{n+1} + w_z^{n+1}) / \Delta t
\end{aligned} \tag{4}$$

2.2 Third Order Upwind Difference and Boundary Conditions

On the free surface, the fluid particle moves by

$$\frac{\partial h}{\partial t} + u \frac{\partial h}{\partial x} - w = 0 \Big|_{z=\tau} \tag{5}$$

The use of kinematic free surface boundary condition makes it possible to employ a higher finite difference scheme. The condition can be written as follows:

$$\frac{\partial h_i^{n+1}}{\partial t} + (u_i + \frac{\partial u_i}{\partial z} \Delta h_i) \cdot \frac{\partial h_i^{n+1}}{\partial x} - w_i = 0 \tag{6}$$

where $h = h(x, t)$ represents the elevation.

Expanding in Taylor series, the time-derivative term can be discretized.

$$\frac{\partial h_i^{n+1}}{\partial t} = \frac{1}{2\Delta t} \cdot (h_i^{n+1} - 4h_i^n + 3h_i^{n-1}) \tag{7}$$

For the $\partial h^{n+1}/\partial x$ derivative, the third order upwind difference(TOUD) is adopted.

$$c \frac{\partial h}{\partial x} = c \frac{1}{6\Delta x} (-2h_{i-3} + 9h_{i-2} - 18h_{i-1} + 11h_i) \tag{8}$$

where c is the convective velocity which can be decomposed into two parts. One is the central differencing term whose mathematical expression can be obtained by suitable Taylor expansions as follows:

$$\frac{c}{24\Delta x} (h_{i-3} - 27h_{i-2} + 27h_{i-1} - h_i) \tag{9}$$

The other is the diffusion term, which is the fourth derivative of the velocity.

$$\frac{3c}{8\Delta x} (-h_{i-3} + 7h_{i-2} - 11h_{i-1} + 5h_i) \tag{10}$$

The latter is expected to eliminate the phase shift due to the differentiation. Similarly the third derivative, Eq. (11) also reduces the phase shift and damping.

$$\frac{\alpha c}{(\Delta x)^3} (-h_{i-3} + 3h_{i-2} - 3h_{i-1} + h_i) \tag{11}$$

where $\alpha = -\frac{(\Delta x)^2}{6}$ is a constant.

Eq. (11) is added to the right-hand side term of Equation (10), and the new formulation for the $\partial h/\partial x$ becomes,

$$\begin{aligned}
c \frac{\partial h}{\partial x} = & c \frac{1}{6\Delta x} (-h_{i-3} + 6h_{i-2} - 15h_{i-1} + 10h_i) + \\
& \frac{\alpha c}{(\Delta x)^3} (-h_{i-3} + 3h_{i-2} - 3h_{i-1} + h_i)
\end{aligned} \tag{12}$$

Introducing Eq. (7) and Eq. (12) into Eq. (6), the vertical coordinate increment at each time step is,

$$\Delta h_i^n = \frac{3\Delta x(\Delta h_i^n - h_i^{n-1}) + \Delta t \cdot [6u_i \Delta x + u_i(\Delta h_{i-1}^n - 6\Delta h_i^n + 15\Delta h_{i+1}^n - Q_i^n)]}{9\Delta x + \Delta t \cdot [10u_i + Q_i^n \frac{\partial u}{\partial x} - 6\Delta x \frac{\partial u}{\partial z}]} \quad (13)$$

The expression is of the second order accuracy for $h(0(h^2))$ for any $u > 0$. Q_i^n in Eq. (13) is,

$$Q_i^n = -h_{i-1}^n + 6h_i^n - 15h_{i+1}^n + 10h_i^n \quad (14)$$

The boundary conditions are as follows.

upstream

$$u = 1, v = 0, w = 0 \text{ and } p = 0 \quad (15)$$

$$\Delta u = \Delta v = \Delta w = 0$$

downstream

$$u_i = v_i = w_i = 0 \quad (16)$$

$$\Delta u_i = \Delta v_i = \Delta w_i = \Delta p_i = 0$$

symmetrical

$$u_n = v_n = w_n = 0 \quad (17)$$

$$\Delta u_n = \Delta v_n = \Delta w_n = \Delta p_n = 0$$

body surface

$$u = v = w = 0, p_i = 0 \quad (18)$$

$$\Delta u = \Delta v = \Delta w = 0, \Delta p_i = 0$$

3. Results and Discussion

3.1 Computational Condition

The ratio of span/chord is 3.0 with the shape of NACA 0012 section in the spanwise direction at 10° and 20° angles of attack. The submergence depth is 0.4 and 0.8 respectively. The domain is 3.5 times the chord length in the streamwise direction. All parameters are based on the wing chord L and uniform velocity U_0 . The minimum grid spacing in z direction is 0.002. The flow has been accelerated during the first 500 time steps. Three computational cases are carried out to compare the original MAC case. The condition is that $d/L=0.4$, $\alpha=20^\circ$ for the case A, 0.8, 20° for the case B, and 0.8, 10° for the case C.

The maximum number of iterations per time step is 10 to 50, which depends on the pressure difference between the present and next calculations.

Fig. 1 shows the coordinate system for the computation ; x , y and z represent coordinates in a Cartesian system, x in the uniform flow

direction, y in the lateral and z normal to the x - y plane. Fig. 2 shows the mesh system and computing domain.

3.2 Discussion

The free surface wave profiles are shown in Fig. 3 which presents a comparison between the old(MAC) method and the new numerical scheme at $t=3.0$ where t is the non-dimensionalized time. As can be seen, the free surface wave has reasonably developed by using the new finite difference scheme of the Euler-type formulation. It is a result of the third derivative introduced in the simulation. The new method is on the whole successful, but it is quite conspicuous especially in the shallow submergence case. The effect of angle of attack and submergence depth can be seen in case B and case C. This numerical result demonstrates that the new finite method does not cast a doubt on its validity. Fig. 4 shows the pressure contours computed by the MAC method and the new method. The pressure difference can be seen near the free surface for both cases. However, there is hardly seen any difference near the wing surface. Fig. 5 shows the velocity vectors in the whole domain. Here, (a) and (b) correspond to the midspan section for case A. The velocity defect can be seen clearly for both cases, but the fully generated free surface of (b) makes some differences in the vector direction and magnitude. Fig. 6 shows the velocity vector in y - z plane. The two methods show similar phenomena, i.e., vortical motion around the tip. Fig. 7 shows the pressure coefficient on the wing surface. The dotted line is obtained by the new method. Roughly estimated, the closed area of dotted line is a little bit less than that of old method. It means that there may be some differences between the two methods in the values of drag and lift.

4. Conclusion

(1) The finite difference method with the TOUD

gives the better results in the free surface generation. The wave in the far downstream can be made even if the grid number is so limited.

(2) The free surface wave can be generated at the large angle of attack 20° without divergence. It means that the current N-S solver can simulate free surface viscous flows more efficiently with the TOUD. The computation time is slightly reduced due to the faster generation of the free surface wave.

References

Floryan, J. M. and Rasmussen, H., 1989, "Numerical methods for viscous flow with moving boundaries", *Appl. Mech. Rev.*, Vol. 42, pp. 323~341.

Harlow, F. H. and Welch, J. E., 1965, "Numerical calculation of time dependent viscous incompressible flow of fluid with free surface", *Phys. Fluids*, Vol. 8, pp. 2182~2189.

Miyata, H., 1986, "Finite difference simulation of breaking waves", *J. Comp. Phys.*, Vol. 65, pp. 179~214.

Nichols, B. D. and Hirt, C. W., 1971, "Improved free surface boundary conditions for numerical incompressible flows", *J. Comp. Phys.*, Vol. 8, pp. 434~448.

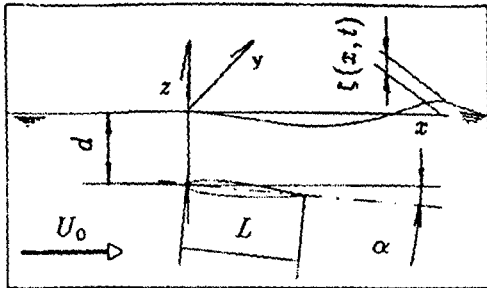


Fig. 1 Definition of coordinate and flow

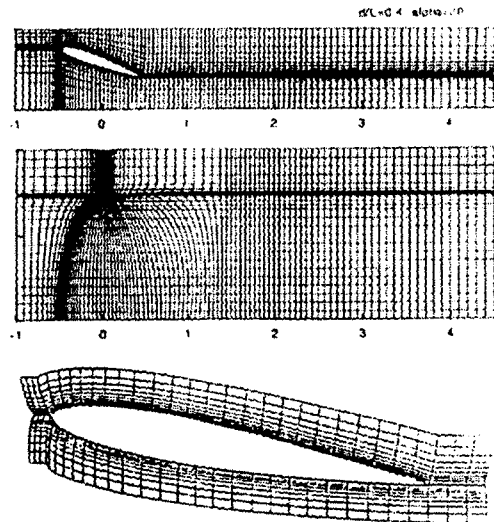
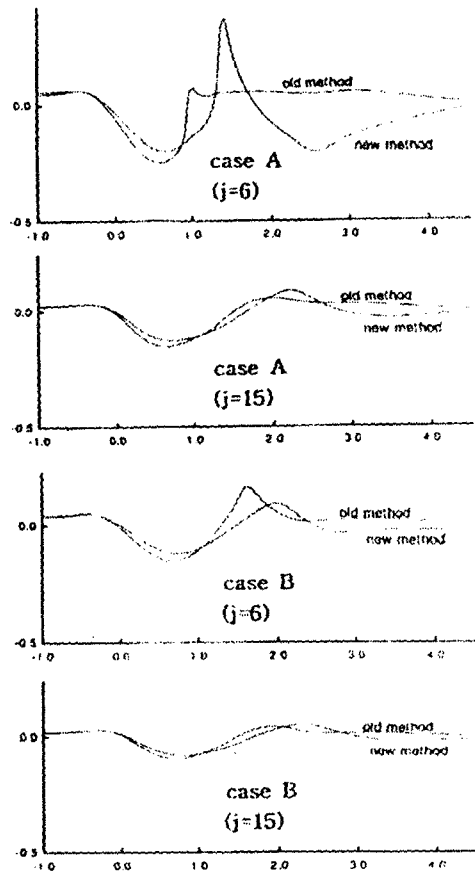


Fig.2 View of grid generation



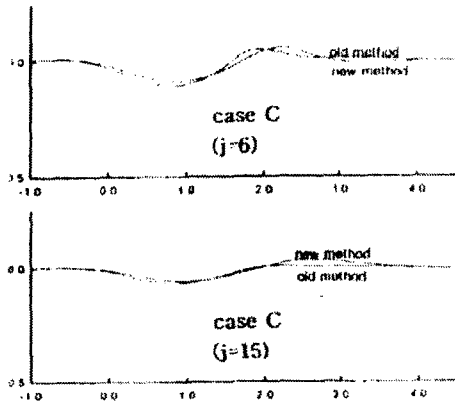


Fig. 3 Free surface development by MAC and new finite difference method

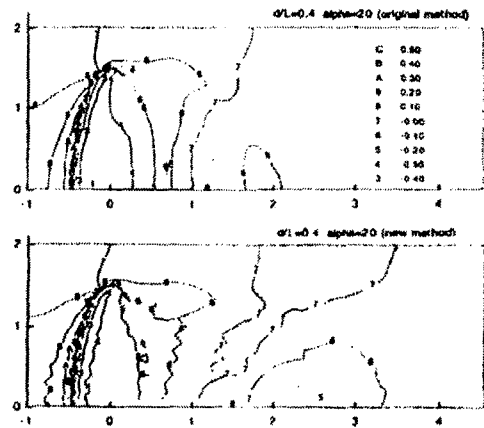


Fig. 5 Pressure contours on the wing surface (upper: suction side, below: pressure side)

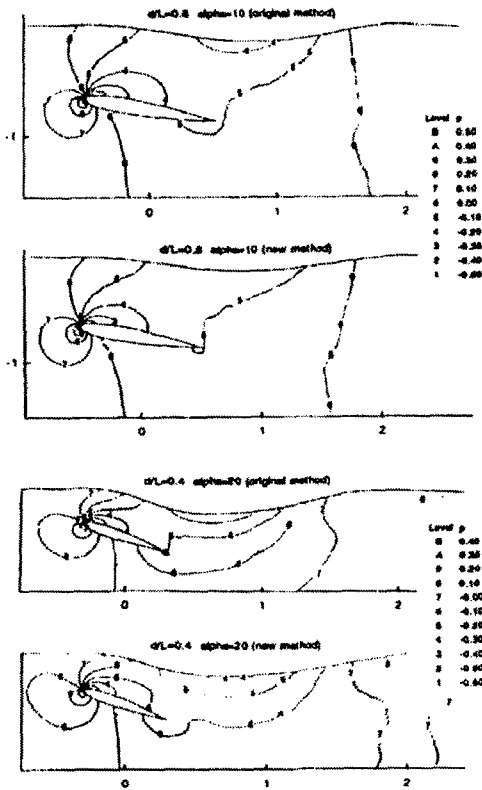


Fig. 4 Pressure development by MAC and new finite difference method

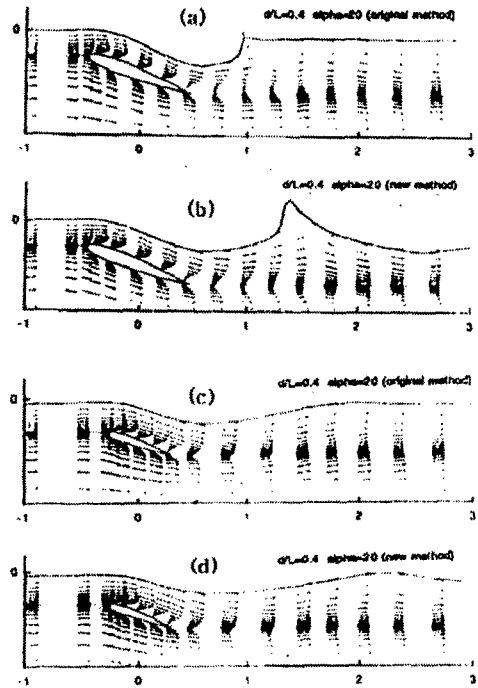


Fig. 6 Spanwise pressure (solid: MAC, dotted: new method)

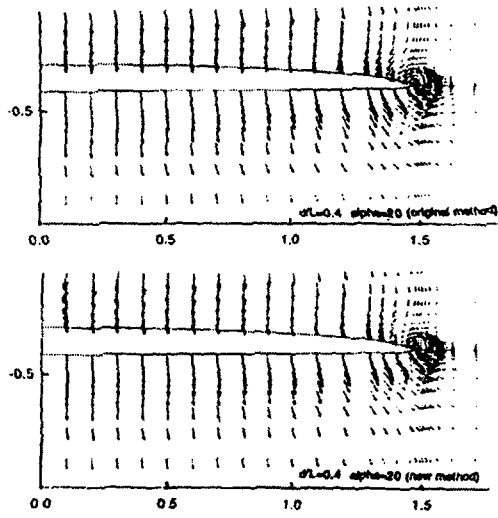


Fig. 7 Velocity vectors (upper: MAC, below: new method)

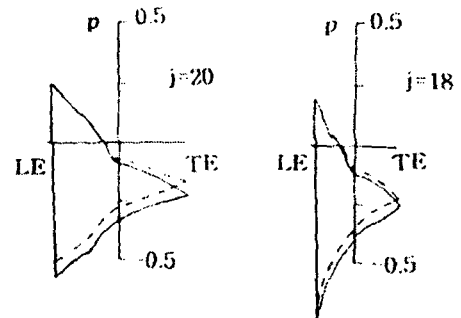
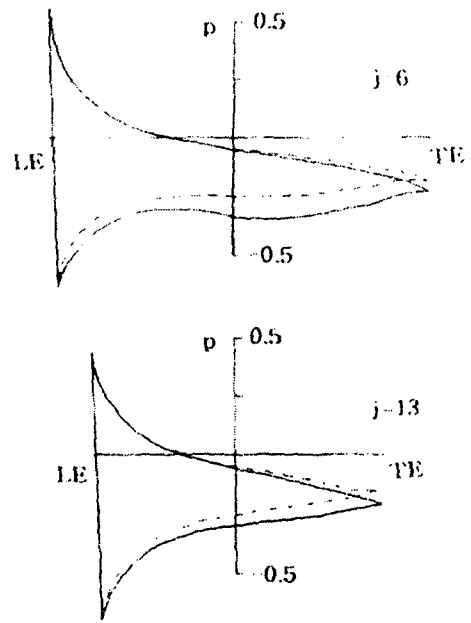


Fig. 8 Spanwise pressure distribution on wing surface (solid line; old method, dotted; new method)